Spectroscopic Methods

DOI: 10.1002/ange.201005402

Single-Molecule Four-Color FRET**

*Jinwoo Lee, Sanghwa Lee, Kaushik Ragunathan, Chirlmin Joo, Taekjip Ha, and Sungchul Hohng**

Single-molecule fluorescence resonance energy transfer (FRET)[1] has provided unprecedented details of fundamental processes in biology.[2] However, information on single interfluorophore distances in conventional two-color FRET is insufficient to capture the intrinsic complexity of many biological systems. To cope with this challenge, single-molecule multicolor FRET techniques have been developed,[3–8] and the capability of three-color FRET detection has been utilized to solve a number of important biological problems.[9–12] As single-molecule FRET approaches are being expanded to include more complex biological systems, there is an ever-increasing demand for more advanced FRET techniques. Here we report the development of a single-molecule four-color FRET technique implemented for both confocal and total internal reflection fluorescence (TIRF) microscopy, which can determine six interfluorophore FRET efficiencies in real time. As proof-of-concept experiments, the technique was used to observe the correlated motions of four arms of the Holliday junction, and to investigate the correlation of RecA-mediated strand exchange events at both ends of a synaptic complex.

Realization of reliable single-molecule four-color FRET requires four fluorophores with high photostability and clear spectral separation. However, it has been impractical to use more than three fluorophores in single-molecule FRET measurements due to pronounced crosstalk between fluorophores limited to the visible range. Recent introduction of highly photostable infrared fluorophore Cy7 to the single-molecule three-color FRET technique opened a new way to realize single-molecule four-color FRET with both negligible spectral overlap and long observation time provided that we find an optimum blue fluorophore with high photostability and clear spectral separation from the dye trio of Cy3–Cy5–Cy7 (550-850 nm).[13] Among candidates of blue fluorophores that we tested (Cy2, Alexa488, Atto488, and DyLight488; see Supporting Information Table 1), we selected Cy2. The key advantages of Cy2 are a small spectral overlap with Cy3 (Supporting Information Figure 1a), and a low probability of a redshifted state (Supporting Information Figure 2). We note that the increased sensitivity of the Cy2–Cy7 FRET pair to distance may be utilized in applications measuring small changes in distance (Supporting Information Figure 1b). In applications requiring longer FRET ranges (Supporting Information Figure 1d) and a longer observation time (Supporting Information Table 2), conventional blue dyes such as Alexa488 may be used (Supporting Information Figure 1c,d), even though multistate behavior of Alexa488 might hinder precise FRET assignment.[14]

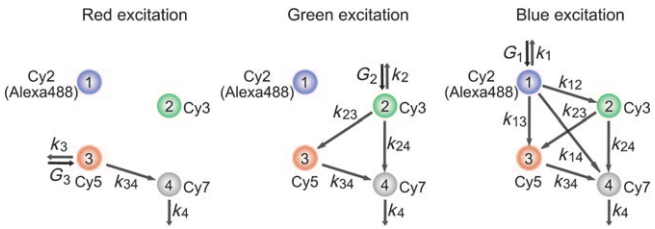

Figure 1. Interaction diagram of four fluorophores, and the alternating laser excitation scheme to determine six interdye FRET efficiencies.

A total of six interdye distances must be determined in four-color FRET. To recover all the information necessary to calculate six interdye distances, we developed an approach using three independent excitation lasers: a red laser (633 or 640 nm) for Cy5, a green laser (532 nm) for Cy3, and a blue laser (473 nm) for Cy2 or Alexa488 (Figure 1). A detailed scheme of the FRET calculation is described in the Supporting Information. Briefly, the FRET efficiency of the Cy5–Cy7 pair (E_{34}) is determined by red excitation (Figure 1, left).

[*] J. Lee,[+] S. Lee,[+] Prof. Dr. S. Hohng
Department of Physics and Astronomy
Department of Biophysics and Chemical Biology
National Center for Creative Research Initiatives
Seoul National University, Seoul 151-747 (Korea)
Fax: (+82) 2-871-8083
E-mail: shohng@snu.ac.kr
K. Ragunathan
Center for Biophysics and Computational Biology
Department of Physics, Center for the Physics of Living Cells
University of Illinois at Urbana-Champaign, Urbana, IL 61801 (USA)
Dr. C. Joo
School of Biological Sciences, Seoul National University
Seoul 151-747 (Korea)
Prof. Dr. T. Ha
Center for Biophysics and Computational Biology
Department of Physics, Center for the Physics of Living Cells
University of Illinois at Urbana-Champaign
Howard Hughes Medical Institute, Urbana, IL 61801 (USA)
[+] These authors contributed equally to this work.

[**] This work was supported by the Creative Research Initiatives (Physical Genetics Laboratory, 2009-0081562), the World Class University project (R31-2009-100320), and the US National Science Foundation grants (0822613 and 0646550). T.H. is an investigator with the Howard Hughes Medical Institute. J.L. was financially supported by a Hi Seoul Science (Humanities) Fellowship from Seoul Scholarship Foundation.
Supporting information (including experimental details) for this article is available on the WWW under http://dx.doi.org/10.1002/anie.201005402.

Next, FRET efficiencies of Cy3–Cy5 (E_{23}) and Cy3–Cy7 (E_{24}) are determined with green excitation on the basis of E_{34} (Figure 1, middle). Finally, the remaining three FRET efficiencies (E_{12}, E_{13}, and E_{14}) are determined with blue excitation on the basis of the three FRET efficiencies that were previously determined (Figure 1, right). The sequential determination of FRET efficiencies in real time was achieved by alternating three excitation lasers on a faster timescale than the conformational dynamics of molecules while synchronizing the detection of fluorescence signals with laser switching. The scheme reported here is distinguished from the previously reported alternating laser excitation (ALEX) method[6,15,16] in that the probe–probe stoichiometries are not determined due to the reduced number of switching lasers to gain a higher time resolution. If need be, ALEX analysis can be incorporated by adding a 730 nm laser to the setup.

We first realized single-molecule four-color FRET in confocal microscopy (Supporting Information Figure 3a). Three excitation lasers (473, 532, and 633 nm) were switched on and off with electro-optic modulators. Switching of the laser lines and detection of fluorescence signals were synchronized with trigger lines of a timer/counter board. We also implemented single-molecule four-color FRET detection in TIRF microscopy, which significantly enhances the yield of data from single-molecule FRET measurements, and is mandatory in studies of irreversible biological processes (Supporting Information Figure 3b). To switch three excitation lasers (473, 532, and 640 nm), we used mechanical shutters with a switching time of 1.5 ms, which did not affect data acquisition at filming rates below 30 frames per second. Laser switching was synchronized with fluorescence imaging by using an electronic circuit containing flip-flops and multiplexers (Supporting Information Figure 4).

The Holliday junction, composed of four helical arms (Figure 2a), exhibits conformational dynamics between two different stacking conformers, isoI and isoII,[17–19] and is thus a good model system for demonstrating the capability of our four-color FRET method (Figure 2b). Figure 2c shows representative fluorescence intensity–time traces of the Holliday junction labeled with Cy2, Cy3, Cy5, and Cy7 at the ends of the four arms as in Figure 2a. From the data obtained by confocal microscopy, all six FRET efficiencies could be calculated as in Figure 2d (black lines), where the overlaid red lines are most probable trajectories generated by hidden Markov modeling (HMM).[20] Consistent with the model in Figure 2b, E_{14} and E_{23} remained in one state, and the other FRET pairs showed two-state fluctuations with correlations and anticorrelations, as expected, that is, all interdye FRET efficiencies can be simultaneously measured and correlated with the conformational dynamics of the Holliday junction. Note that FRET efficiencies determined in the last step (E_{12}, E_{13}, and E_{14}) are subject to higher noise due to error amplification from multiple FRET calculation steps, and thus there sometimes appears to be dynamics, which are not real. The HMM fits obtained while allowing more than two states converged into the two states (Figure 2d), and thus this conclusion is justified. The overall correlation of different FRET pairs is clearly visualized in three-dimensional FRET distributions of E_{12}, E_{13}, and E_{14} (Figure 2e), and of E_{23}, E_{24}, and E_{34} (Figure 2f). The dynamics of the Holliday junction measured by four-color TIRF microscopy was identical to that observed by using confocal microscopy (Supporting Information Figure 5).

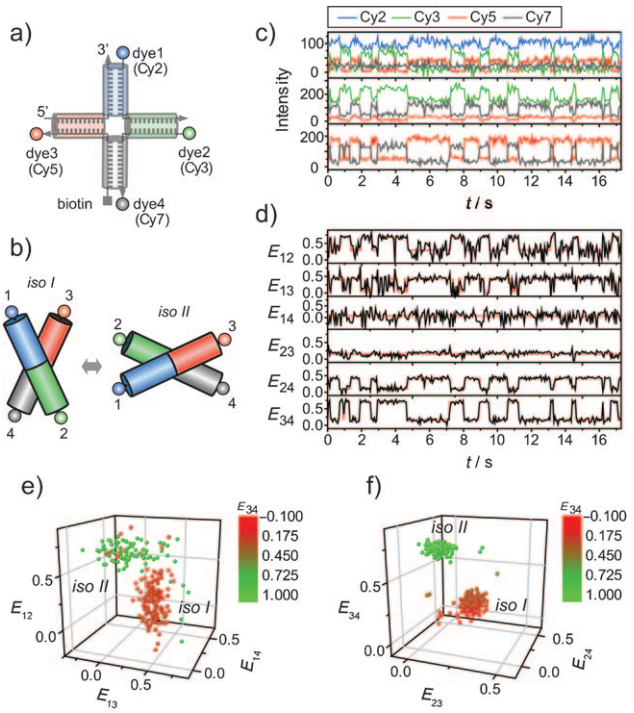

Figure 2. Holliday junction dynamics observed by single-molecule four-color FRET. a) Labeling scheme. b) Conformational dynamics model of the Holliday junction. c) Representative fluorescence intensity–time traces for blue (top), green (middle), and red excitations (bottom). Fluorescence signals of Cy2, Cy3, Cy5, and Cy7 are colored blue, green, red, and gray, respectively. In the top panel, the Cy2 signal is vertically shifted for clear visualization. d) FRET efficiency–time traces. The six FRET efficiencies (black lines) were calculated from the data in (c) by following the method described in the Supporting Information. Red lines are the most probable FRET trajectories generated by hidden Markov modeling. e) Three-dimensional distribution of E_{12}, E_{13}, and E_{14} of (d). f) Three-dimensional distribution of E_{34}, E_{23}, and E_{24} of (d). To make a connection between (e) and (f), each data point in the plots is color-coded on the basis of E_{34}.

In conventional FRET experiments, it is difficult to correlate the kinetics of two events spatially separated by a distance well beyond the FRET range (>10 nm). With four-color detection capability, we can implement a "dual FRET pair" scheme, in which two independent FRET pairs measure the correlation between two spatially well separated events and determine their simultaneity. As a demonstration, we performed RecA-mediated strand-exchange experiments.[21,22] A partial double-stranded DNA labeled with two acceptors (Cy5 at the junction and Cy7 at the terminal end of a 70-nt single-stranded DNA) was immobilized on a polymer-coated quartz surface. After forming a RecA filament, we injected homologous double-stranded DNA, the ends of which were labeled with two donors (Alexa488 and Cy3). In this scheme, the docking of double-stranded DNA to the immobilized RecA filament is observed as an abrupt appearance of fluorescence signal, and the propagation of

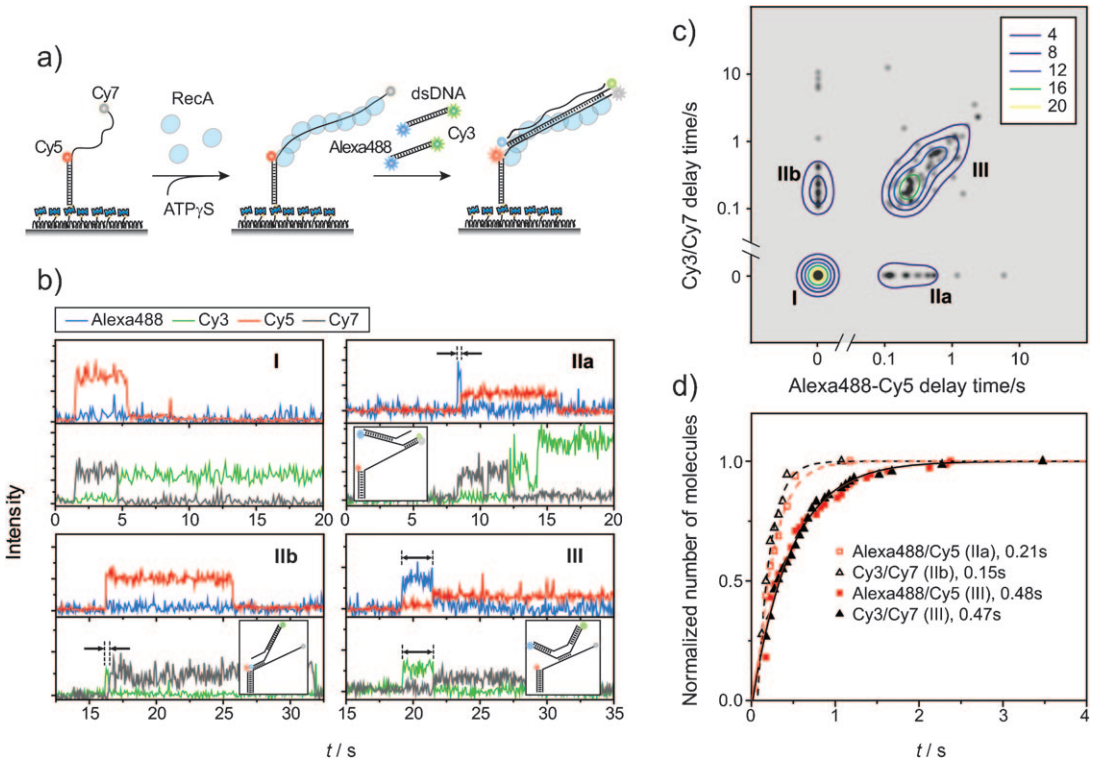

Figure 3. RecA-mediated strand-exchange experiments. a) Schematic diagram of the experiments. b) Representative fluorescence intensity–time traces of strand exchange. In each plot, the top panel shows the intensity trace of Alexa488 (blue lines) and that of Cy5 (red lines) with 473 nm excitation, and the bottom panel shows Cy3 (green lines) and Cy7 (gray lines) signals with 532 nm excitation. Delay times and corresponding models of strand-exchange initiation are shown in the figure. c) Relative distribution of delay times at both ends of the synaptic complex from 135 molecules. To visualize the distribution of delay times, each data point is represented as a gray-scaled 2D Gaussian distribution. A contour plot of population density is overlaid for clear visualization of the three species. d) Cumulative probability distributions of the delay times of each species. By fitting the distributions to single exponential functions, delay times required for the completion of strand exchange were obtained.

strand exchange as the subsequent evolution of FRET (Figure 3a). In the reaction product, high FRET of Alexa488–Cy5 and Cy3–Cy7 pairs reports completion of strand exchange at each end of the DNA.

Representative single-molecule intensity–time traces measured in TIRF microscopy show that high FRET at each end is achieved either directly upon docking or after a delay, and thus we can classify molecules into three categories: Type I (17% of 135 molecules) did not show any delay between docking and completion of strand exchange at either end; Types IIa (13%) and IIb (16%) showed a delay only at one of the two ends; and Type III (54%) showed a delay at both ends (Figure 3b). The correlation plot of E_{24} versus E_{13} at the moment of docking more clearly shows the existence of the four distinct populations, which later merge into one population with high values for both E_{24} and E_{13} (Supporting Information Figure 6). Our systematic two-color FRET analysis showed that the zero delay corresponds to strand exchange beginning from the labeled end.[23] Our four-color results demonstrate that the initiation of strand exchange can occur from the ends of DNA (Types IIa and IIb), or from the middle (Type III). This conclusion could not be directly reached from the two-color FRET measurements, since it was not possible to monitor events at both ends of single RecA synaptic complexes. Furthermore, the dual FRET measurements reveal a number of surprising observations which two-color FRET cannot provide: 1) Strand exchange events which initiated from the middle showed a strong correlation between the two delay times (Figure 3c, Type III), and 2) these events are completed more slowly than those which initiated from the ends (Figure 3d). The existence of Type I species was also unexpected from two-color FRET analysis, and implies diverse paths of strand-exchange initiation. More systematic studies varying DNA sequence, length, and labeling positions would be needed for a complete understanding of this remarkably complex process.

In summary, we have realized a reliable single-molecule four-color FRET technique that can determine six interfluorophore FRET efficiencies in real time. While three-color FRET monitors three distances, our method doubles the number of observables. It is also robust even in the presence of FRET interactions between all four fluorophores as we demonstrated for the dynamics of the Holliday junction. The experiments with RecA demonstrate the strength of a multidimensional analysis measuring two independent reaction coordinates simultaneously for a single molecule. We expect that the technique reported here will have broad applications in measuring the correlated dynamics of complex biological systems.[24]

Received: August 30, 2010
Published online: November 23, 2010

Keywords: conformational dynamics · DNA structures · fluorescence · FRET · single-molecule studies

[1] T. Ha, T. Enderle, D. F. Ogletree, D. S. Chemla, P. R. Selvin, S. Weiss, *Proc. Natl. Acad. Sci. USA* **1996**, *93*, 6264 – 6268.
[2] R. Roy, S. Hohng, T. Ha, *Nat. Methods* **2008**, *5*, 507 – 516.
[3] S. Hohng, C. Joo, T. Ha, *Biophys. J.* **2004**, *87*, 1328 – 1337.
[4] M. Heilemann, P. Tinnefeld, G. S. Mosteiro, M. Garcia Parajo, N. F. Van Hulst, M. Sauer, *J. Am. Chem. Soc.* **2004**, *126*, 6514 – 6515.
[5] J. P. Clamme, A. A. Deniz, *ChemPhysChem* **2005**, *6*, 74 – 77.
[6] N. K. Lee, A. N. Kapanidis, H. R. Koh, Y. Korlann, S. O. Ho, Y. Kim, N. Gassman, S. K. Kim, S. Weiss, *Biophys. J.* **2007**, *92*, 303 – 312.
[7] J. Ross, P. Buschkamp, D. Fetting, A. Donnermeyer, C. M. Roth, P. Tinnefeld, *J. Phys. Chem. B* **2007**, *111*, 321 – 326.
[8] B. Person, I. H. Stein, C. Steinhauer, J. Vogelsang, P. Tinnefeld, *ChemPhysChem* **2009**, *10*, 1455 – 1460.
[9] N. K. Lee, H. R. Koh, K. Y. Han, S. K. Kim, *J. Am. Chem. Soc.* **2007**, *129*, 15526 – 15534.
[10] R. Roy, A. G. Kozlov, T. M. Lohman, T. Ha, *Nature* **2009**, *461*, 1092 – 1097.
[11] J. B. Munro, R. B. Altman, C. Tung, J. H. D. Cate, K. Y. Sanbonmatsu, S. C. Blanchard, *Proc. Natl. Acad. Sci. USA* **2010**, *107*, 709 – 714.
[12] N. K. Lee, H. R. Koh, K. Y. Han, J. Lee, S. K. Kim, *Chem. Commun.* **2010**, *46*, 4683 – 4685.
[13] S. Lee, J. Lee, S. Hohng, *PLoS One* **2010**, *5*, e12270.
[14] H. S. Chung, J. M. Louis, W. A. Eaton, *Biophys. J.* **2010**, *98*, 696 – 706.
[15] E. Margeat, A. N. Kapanidis, P. Tinnefeld, Y. Wang, J. Mukhopadhyay, R. H. Ebright, S. Weiss, *Biophys. J.* **2006**, *90*, 1419 – 1431.
[16] A. N. Kapanidis, N. K. Lee, T. A. Laurence, S. Doose, E. Margeat, S. Weiss, *Proc. Natl. Acad. Sci. USA* **2004**, *101*, 8936 – 8941.
[17] S. A. McKinney, A. C. Declais, D. M. J. Lilley, T. Ha, *Nat. Struct. Biol.* **2003**, *10*, 93 – 97.
[18] C. Joo, S. A. McKinney, D. M. J. Lilley, T. Ha, *J. Mol. Biol.* **2004**, *341*, 739 – 751.
[19] S. Hohng, R. Zhou, M. K. Nahas, J. Yu, K. Schulten, D. M. J. Lilley, T. Ha, *Science* **2007**, *318*, 279 – 283.
[20] S. A. McKinney, C. Joo, T. Ha, *Biophys. J.* **2006**, *91*, 1941 – 1951.
[21] S. C. Kowalczykowski, *Nature* **2008**, *453*, 463 – 466.
[22] T. van der Heijden, M. Modesti, S. Hage, R. Kanaar, C. Wyman, C. Dekker, *Mol. Cell* **2008**, *30*, 530 – 538.
[23] K. Ragunathan, C. Joo, T. Ha, unpublished results.
[24] S. Uemura, C. E. Aitken, J. Korlach, B. A. Flusberg, S. W. Turner, J. D. Puglisi, *Nature* **2010**, *464*, 1012 – 1017.

